PROCEEDINGS OF SPIE

SPIEDigitalLibrary.org/conference-proceedings-of-spie

Zero-valent Au, Cu, and Sn intercalation into GeS nanoribbons: tailoring ultrafast photoconductive response

Kushnir, Kateryna, Shi, Teng, Damian, Leticia, Anilao, Auddy, Koski, Kristie, et al.

Kateryna Kushnir, Teng Shi, Leticia Damian, Auddy Anilao II, Kristie J. Koski, Lyubov V. Titova, "Zero-valent Au, Cu, and Sn intercalation into GeS nanoribbons: tailoring ultrafast photoconductive response," Proc. SPIE 11278, Ultrafast Phenomena and Nanophotonics XXIV, 112780I (27 February 2020); doi: 10.1117/12.2546691



Event: SPIE OPTO, 2020, San Francisco, California, United States

Zero-valent Au, Cu and Sn Intercalation into GeS Nanoribbons: Tailoring Ultrafast Photoconductive Response

Kateryna Kushnir*^a, Teng Shi^a, Leticia Damian^{a,b}, Auddy Anilao II^c, Kristie J. Koski^c and Lyubov V. Titova^a

^a Department of Physics, Worcester Polytechnic Institute, Worcester, Massachusetts 01609, USA, ^bCalifornia State University San Marcos, San Marcos, California 92069, USA, ^cDepartment of Chemistry, University of California Davis, Davis, California 95616, USA *E-mail: kkushnir@wpi.edu

ABSTRACT

Germanium sulfide (GeS) is a 2D semiconductor with high carrier mobility and a moderate band gap (~1.5 eV for multilayer crystals), which holds promise for high-speed optoelectronics and energy conversion. Here, we use time-resolved THz spectroscopy to investigate how intercalation of Au, Cu, and Sn impacts the photoexcited carrier dynamics and transient photoconductivity of GeS nanoribbons. We find that zero-valent metals affect the photoexcited carrier lifetime and mobility in different ways. Intercalation of GeS with Cu reduces the lifetime of carriers from ~ 120 ps to 60 ps, while Au and Sn intercalation do not. At the same time, intercalation with Cu, Sn and Au significantly enhances the scattering time of photoexcited carriers (~120 fs vs ~65 fs without intercalation), highlighting the potential of zero-valent metal intercalation as a tool for engineering the optoelectronic properties of GeS nanostructures for application in high-speed electronic devices.

Keywords: terahertz spectroscopy, photoconductivity, ultrafast carrier dynamics, semiconductor, intercalation, germanium sulfide

1. INTRODUCTION

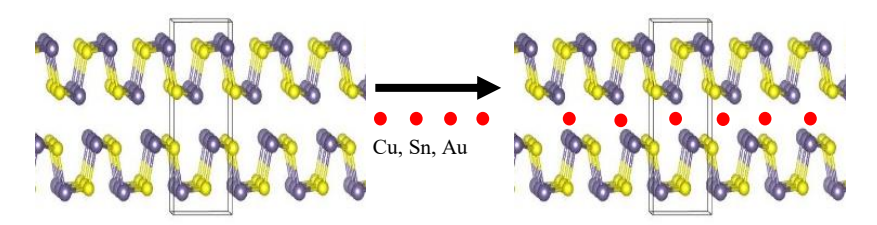


Figure 1 Schematic for intercalation in the GeS, where guest species Cu, Sn and Au can be inserted into the van der Waals gap.

In the past few decades, two-dimensional (2D) nanomaterials have attracted much attention due to their unique electronic and optical properties.[1, 2] They exhibit a wide range of electronic band structures, from insulators and topological insulators to semiconductors, metals, and superconductors.[3-6] Recently, various methods to modify 2D materials to achieve tunable properties and device performance have experienced rapid development. Among them is the ability to insert molecules, ions, and atoms between the layers of material with weak van der Waals interactions. [3] (Fig. 1). Intercalation has arisen as a powerful tool to significantly increase the doping level and change the phase of the 2D material, either permanently or reversibly. Engineering electronic, optical, thermal, magnetic, and catalytic

Ultrafast Phenomena and Nanophotonics XXIV, edited by Markus Betz, Abdulhakem Y. Elezzabi, Proc. of SPIE Vol. 11278, 112780I · © 2020 SPIE CCC code: 0277-786X/20/\$21 · doi: 10.1117/12.2546691

properties of 2D via intercalation is advantageous for optoelectronics, superconductors, thermoelectronics, catalysis and energy storage applications.[7-16]

GeS is a 2D van der Waals semiconductor with high carrier mobility and a moderate band gap (~1.5 eV in the bulk), which holds promise for high-speed optoelectronics and energy conversion.[17-19] Theory predicts that GeS monolayers are multiferroic, combining a robust ferroelasticity and ferroelectric polarization at room temperature.[20, 21] In-plane electric polarization results from an elastic distortion of the lattice, as the top and the bottom atoms shift in the armchair direction.[21, 22] It is predicted to result in a pronounced shift current effect, which is a major mechanism behind the bulk photovoltaic effect (BPVE) and makes GeS a promising candidate for BPVE-based solar cells.[17, 20, 21, 23, 24] In our earlier work, we have experimentally verified the prediction of a shift current in GeS by observing THz emission due to the surface shift current in GeS nanoribbons.[18] Here, we explore the possibility of tuning the electronic properties and photoexcited carrier dynamics in this material by intercalation of zero-valent metals, such as Cu, Sn and Au.[25-27] We use time-resolved THz spectroscopy (TRTS), a noncontact probe of microscopic photoconductivity, to investigate how intercalation of zero-valent metals impacts the lifetime and mobility of the photoexcited charge carriers.[28-33]

2. EXPERIMENTAL SECTION

Sample preparation. GeS nanoribbons on a sapphire substrate were prepared using established vapor—liquid—solid (VLS) growth. GeS nanoribbons vary from 10 to 100 μm in length and 1–100 μm in width, as well as 30–50 nm in thickness.[34] Zero-valent intercalation occurs through the generation of dilute amounts of metal atoms in solution, such as through a disproportionation redox reaction following established chemistries.[27, 35, 36] The initial pH of all glassware was controlled before use by cleaning in an acid bath, followed by neutralization overnight in deionized water.[27] The pretreatment of the glassware has a significant effect on both intercalation and deintercalation, especially of copper. Zero-valent metals were then intercalated through a disproportionation redox reaction.[27, 35] In the case of Cu, intercalation was performed by dissolving an air-stable Cu¹⁺ salt of 0.01 g of tetrakis (acetonitrile) copper(I) hexafluorophosphate in 5 mL of HPLC grade acetone. The substrate with 2D materials was placed in a flask with the prepared acetone solution just below reflux at 45 °C for 3 hours. Intercalation of Sn was performed by dissolving 0.01 g of SnCl₂ together with 0.1 g of tartaric acid in 5 mL of HPLC acetone. The substrate with the sample was placed in a flask with precursor solution and kept at 45 °C for 2 hours.

Time-resolved THz spectroscopy. GeS nanoribbons were optically excited with 800 nm, 100 fs pulses. THz probe pulses with a 0.3 - 2 THz bandwidth, corresponding to 1-8 meV energy range, were generated and detected in 1 mm - thick ZnTe crystals. The changes in amplitude and phase of the transmitted THz pulses through a photoexcited sample (\vec{E}_g) were compared to those transmitted through an unexcited sample (\vec{E}_g), and were used to extract the complex photoconductivity as: [28]

$$\frac{\tilde{E}_{S}(\omega)}{\tilde{E}_{O}(\omega)} = \frac{1+N}{1+N+Z_{O}\hat{\sigma}(\omega)d},\tag{1}$$

where $Z_0 = 377 \Omega$ is the impedance of the free space, N is the refractive index of the substrate in the THz range, and d is the thickness of the optically excited region ($d \ll \lambda \text{ or } n_s \omega d/c \ll 1$).

3. RESULTS AND DISCUSSION

Photoconductivity dynamics after excitation with 800 nm, 100 fs pulses were studied in pure GeS nanoribbons and in GeS nanoribbons intercalated with Cu, Sn and Au. The atomic percent of intercalated metals in GeS, as previously mentioned, is limited to \sim 3% due to its corrugated structure hindering intercalation. [25] Photoconductivity can be represented by a transient change in the THz probe pulse peak. Normalized transient photoconductivity for GeS nanoribbons and GeS nanoribbons intercalated with \sim 3% atomic percent of Au, Cu and Sn following excitation with 445 μ Jcm⁻² is shown in Fig. 2. It exhibits a fast onset followed by a decay over hundreds of picoseconds. We note

here that 800 nm (1.55 eV) excitation of GeS, unlike 400 nm (3.1 eV) excitation, does not result in THz emission, indicating that 800 nm pulses predominantly excite carriers deep within the multilayer nanoribbons rather that in the surface layer which is responsible for THz emission by ultrafast shift current.

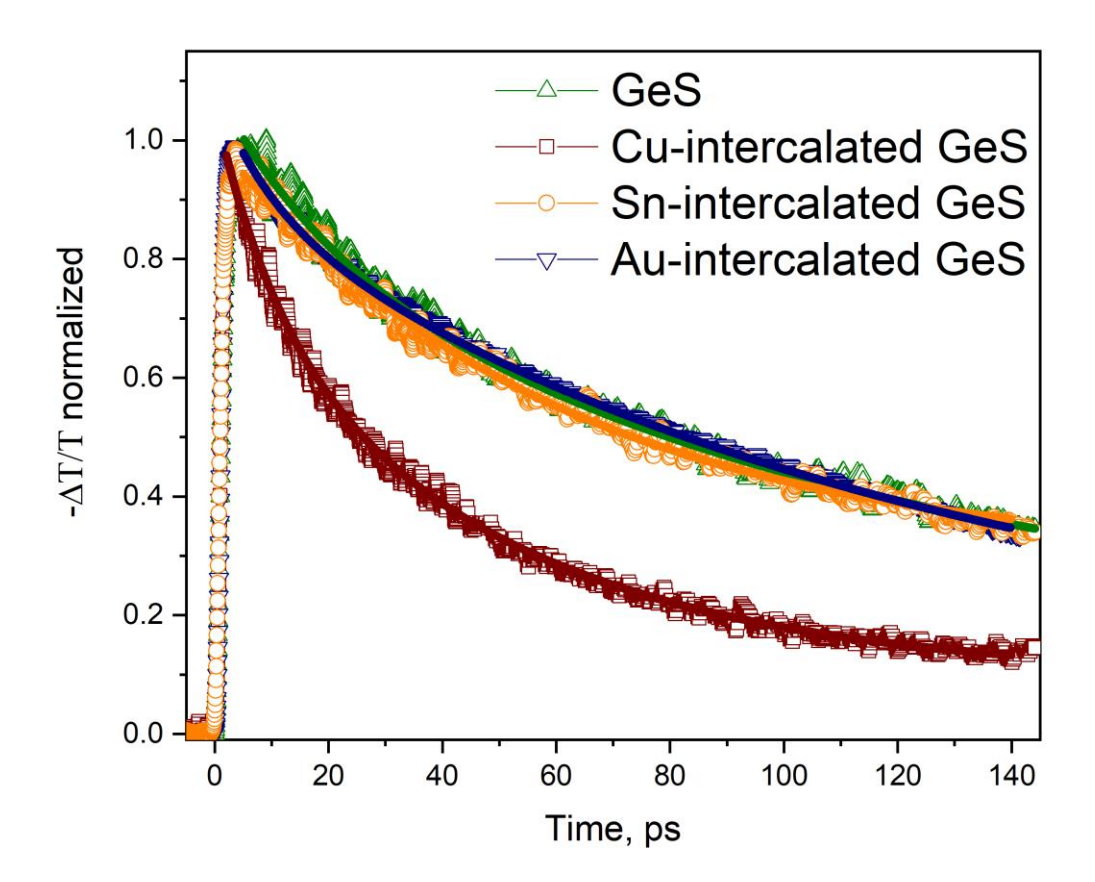


Figure 2. Photoconductivity dynamics: normalized change in THz peak transmission in GeS nanoribbons, and GeS nanoribbons intercalated with Cu, Sn and Au, following photoexcitation with 800 nm, $\sim 100 \text{ fs pulses}$.

We find that photoconductivity dynamics are not significantly affected by either Au or Sn intercalation, as GeS, GeS:Au and GeS:Sn nanoribbons exhibit photoconductivity that initially decays over ~ 60 ps time scales with a much longer lived component. Photoconductivity decays as free photoexcited carriers become trapped at the defect state, both in the bulk and at the nanoribbon edges, and eventually recombine. On the other hand, intercalation with Cu significantly decreases carrier life time, as it introduces a much faster, ~ 10 ps decay component. We hypothesize that Cu intercalation introduces interband states that act as efficient traps for photoexcited carriers, while the Au- and Sn-intercalation does not.

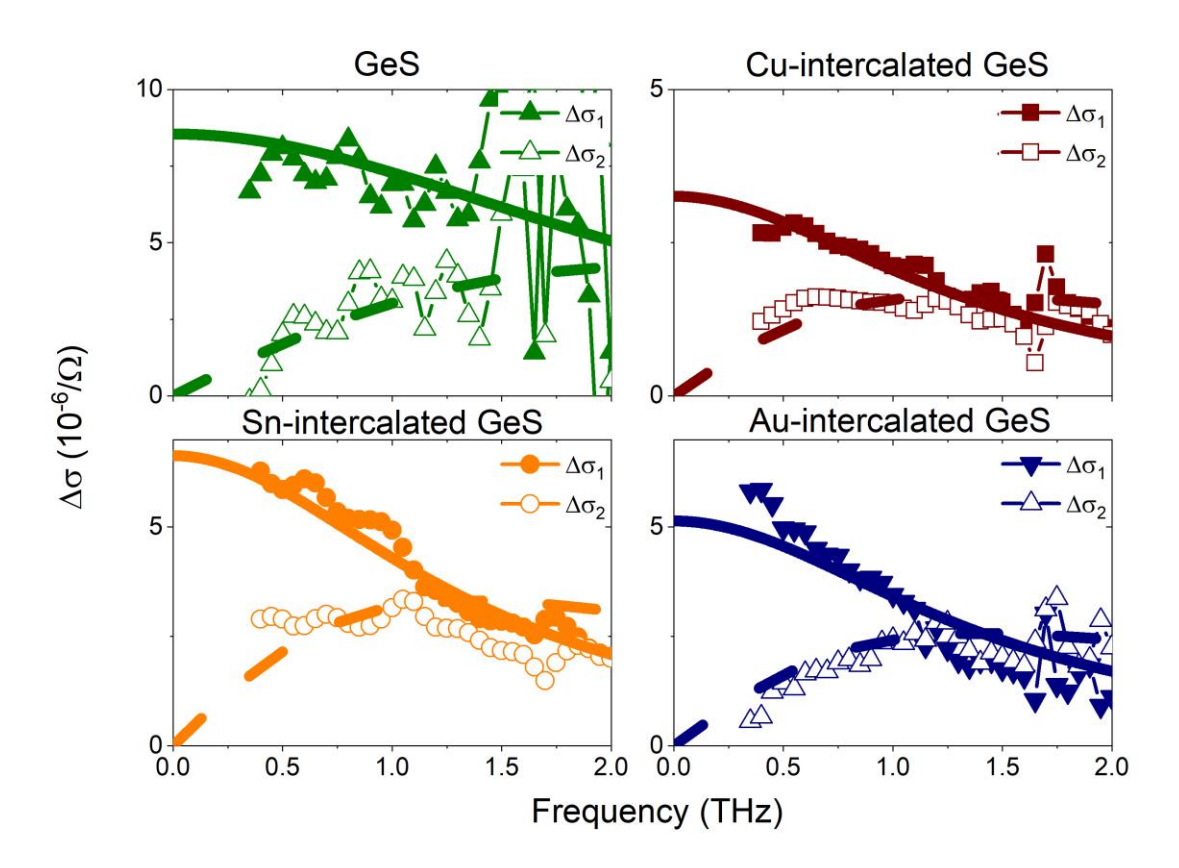


Figure 3. Real ($\Delta\sigma_1$) and imaginary ($\Delta\sigma_2$) components of THz photoconductivity of GeS nanoribbons, Cu -, Sn – and Au-intercalated GeS nanoribbons respectively, measured at 5 ps after the excitation. The lines represent global fit for real and imaginary components of the conductivity to the Drude model.

In addition to providing information about free carrier lifetimes after photoexcitation, TRTS allows us to measure frequency resolved complex THz photoconductivity. Photoexcitation-induced changes in the amplitude and phase of the THz pulse waveform transmitted through the sample were used to extract complex photoinduced changes in conductivity 5 ps after excitation with 445 μ J/cm², 800 nm pulses. [18, 28, 29, 37, 38] Real ($\Delta\sigma_1$) and imaginary ($\Delta\sigma_2$) photoconductivity components are plotted in Fig. 5 as a function of THz frequency (ω). In general, the complex conductivity ($\hat{\sigma}$) of both samples is well described by the Drude model, Equation (2), where N is the charge carrier density, m* is the effective carrier mass, and τ_D is the effective scattering time:[30-32, 38-44]

$$\hat{\sigma}(\omega) = \frac{Ne^2 \tau_D / m^*}{1 - i\omega \tau_D} \tag{2}$$

The τ_D was first determined by fitting the measured frequency-resolved complex conductivity to the model. We find that the effective scattering times for all intercalated samples almost doubled in comparison to the pure GeS, as $\tau_D \approx 65 \ fs$ in pure nanoribbons and $\tau_D \approx 120 \ fs$ in GeS nanoribbons intercalated with either one of the zero valent metals Au, Sn, Cu The effective carrier scattering time, which determines carrier mobility, includes contributions from all possible carrier scattering processes, such as scattering by defects, interfaces, phonons, and carrier-carrier scattering at high carrier densities. Among these, the mechanism most susceptible to intercalation-induced changes is carrier-phonon scattering, as subtle changes to the host lattice can result in either softening or stiffening phonon modes. [45, 46] Previously reported XRD measurements reveal that zero valent metal intercalation increases the unit

cell volume, primarily due to a slight increase in the lattice constants in the armchair and, to a lesser effect, the zigzag direction.[25] Deformation of the lattice within the 2D layers due to intercalation may have an impact on the phonon modes.

4. CONCLUSION

We have investigated the influence of zero-valent metal intercalation on the photoconductivity of GeS nanoribbons using time-resolved THz spectroscopy. We find that intercalation can influence two parameters, free carrier lifetime and carrier scattering time. While the scattering time (and, therefore, carrier mobility) is increased by the presence of either Cu, Au or Sn, intercalation of 3% Cu also has a pronounced effect of decreasing the lifetime of photoexcited carriers. In summary, metal intercalation is a promising approach to engineering the microscopic conductivity and photoexcited carrier lifetime in GeS for applications in high-speed electronic devices.

ACKNOWLEDGMENTS

This work was supported by NSF DMR 1750944. L.D. acknowledges support from NSF EEC 1852447 (REU Site) and the McNair Foundation.

REFERENCES

- [1] H. Zhang, "Ultrathin Two-Dimensional Nanomaterials," ACS Nano, 9(10), 9451-9469 (2015).
- [2] C. Tan, X. Cao, X.-J. Wu *et al.*, "Recent Advances in Ultrathin Two-Dimensional Nanomaterials," Chemical Reviews, 117(9), 6225-6331 (2017).
- [3] M. Chhowalla, H. S. Shin, G. Eda *et al.*, "The chemistry of two-dimensional layered transition metal dichalcogenide nanosheets," Nature Chemistry, 5(4), 263-275 (2013).
- [4] H. Peng, K. Lai, D. Kong *et al.*, "Aharonov–Bohm interference in topological insulator nanoribbons," Nature Materials, 9(3), 225-229 (2010).
- [5] Y. Li, J. L. Huang, and C. M. Lieber, "Temperaure dependence of the energy gap in \$\{\mathrm{Bi}}_{2}\$\$\{\mathrm{Sr}}_{2}\$\${\mathrm{CaCu}}_{2}\$\${\mathrm{O}}_{8}\$ superconductors by high-resolution electron-energy-loss spectroscopy," Physical Review Letters, 68(21), 3240-3243 (1992).
- [6] J. J. Cha, and Y. Cui, "The surface surfaces," Nature Nanotechnology, 7(2), 85-86 (2012).
- [7] J. Wan, S. D. Lacey, J. Dai *et al.*, "Tuning two-dimensional nanomaterials by intercalation: materials, properties and applications," Chemical Society Reviews, 45(24), 6742-6765 (2016).
- [8] Y. Jung, Y. Zhou, and J. J. Cha, "Intercalation in two-dimensional transition metal chalcogenides," Inorganic Chemistry Frontiers, 3(4), 452-463 (2016).
- [9] M. S. Dresselhaus, "Intercalation In Layered Materials," MRS Bulletin, 12(3), 24-28 (1987).
- [10] F. R. Gamble, J. H. Osiecki, M. Cais *et al.*, "Intercalation Complexes of Lewis Bases and Layered Sulfides: A Large Class of New Superconductors," 174(4008), 493-497 (1971).
- [11] D. E. Prober, M. R. Beasley, and R. E. Schwall, "Fluctuation-induced diamagnetism and dimensionality in superconducting layered compounds: TaS₂(pyridine)₁₂ and NbSe₂," Physical Review B, 15, 5245-5261 (1977).
- [12] Y. Gong, H. Yuan, C.-L. Wu *et al.*, "Spatially controlled doping of two-dimensional SnS2 through intercalation for electronics," Nature Nanotechnology, 13(4), 294-299 (2018).
- [13] J. Yao, K. J. Koski, W. Luo *et al.*, "Optical transmission enhacement through chemically tuned two-dimensional bismuth chalcogenide nanoplates," Nature Communications, 5(1), 5670 (2014).
- [14] R. Liu, C. Wang, Y. Li *et al.*, "Intercalating copper into layered TaS2 van der Waals gaps," RSC Advances, 7(74), 46699-46703 (2017).
- [15] J. N. Coleman, M. Lotya, A. O'Neill *et al.*, "Two-Dimensional Nanosheets Produced by Liquid Exfoliation of Layered Materials," 331(6017), 568-571 (2011).
- [16] F. Withers, H. Yang, L. Britnell *et al.*, "Heterostructures Produced from Nanosheet-Based Inks," Nano Letters, 14(7), 3987-3992 (2014).

- [17] R. Fei, W. Li, J. Li *et al.*, "Giant piezoelectricity of monolayer group IV monochalcogenides: SnSe, SnS, GeSe, and GeS," 107(17), 173104 (2015).
- [18] K. Kushnir, M. Wang, P. D. Fitzgerald *et al.*, "Ultrafast Zero-Bias Photocurrent in GeS Nanosheets: Promise for Photovoltaics," ACS Energy Letters, 2(6), 1429-1434 (2017).
- [19] W.-J. Lee, J. W. Ma, J. M. Bae *et al.*, "Strongly enhanced THz emission caused by localized surface charges in semiconducting Germanium nanowires," Scientific reports, 3, 1984-1984 (2013).
- [20] T. Rangel, B. M. Fregoso, B. S. Mendoza *et al.*, "Large Bulk Photovoltaic Effect and Spontaneous Polarization of Single-Layer Monochalcogenides," Physical Review Letters, 119(6), 067402 (2017).
- [21] A. M. Cook, M. F. B, F. de Juan *et al.*, "Design principles for shift current photovoltaics," Nat Commun, 8, 14176 (2017).
- [22] R. Fei, W. Kang, and L. Yang, "Ferroelectricity and Phase Transitions in Monolayer Group-IV Monochalcogenides," Physical Review Letters, 117(9), 097601 (2016).
- [23] S. R. Panday, and B. M. Fregoso, "Strong second harmonic generation in two-dimensional ferroelectric IV-monochalcogenides," Journal of Physics-Condensed Matter, 29(43), (2017).
- [24] M. Wu, and X. C. Zeng, "Intrinsic Ferroelasticity and/or Multiferroicity in Two-Dimensional Phosphorene and Phosphorene Analogues," Nano Letters, 16(5), 3236-3241 (2016).
- [25] M. Wang, I. Al-Dhahir, J. Appiah *et al.*, "Deintercalation of Zero-Valent Metals from Two-Dimensional Layered Chalcogenides," Chemistry of Materials, 29(4), 1650-1655 (2017).
- [26] H. Yuan, H. Wang, and Y. Cui, "Two-Dimensional Layered Chalcogenides: From Rational Synthesis to Property Control via Orbital Occupation and Electron Filling," Accounts of Chemical Research, 48(1), 81-90 (2015).
- [27] K. J. Koski, J. J. Cha, B. W. Reed *et al.*, "High-Density Chemical Intercalation of Zero-Valent Copper into Bi2Se3 Nanoribbons," Journal of the American Chemical Society, 134(18), 7584-7587 (2012).
- [28] F. A. Hegmann, O. Ostroverkhova, and D. G. Cooke, [Probing Organic Semiconductors with Terahertz Pulses] Wiley-VCH Verlag GmbH & Co. KGaA, (2006).
- [29] P. U. Jepsen, D. G. Cooke, and M. Koch, "Terahertz spectroscopy and imaging–Modern techniques and applications," Laser & Photonics Reviews, 5(1), 124-166 (2011).
- [30] Z. Mics, A. D'Angio, S. A. Jensen *et al.*, "Density-dependent electron scattering in photoexcited GaAs in strongly diffusive regime," Applied Physics Letters, 102(23), 231120 (2013).
- [31] C. A. Schmuttenmaer, "Exploring Dynamics in the Far-Infrared with Terahertz Spectroscopy," Chemical Reviews, 104(4), 1759-1780 (2004).
- [32] J. R. Knab, X. Lu, F. A. Vallejo *et al.*, "Ultrafast Carrier Dynamics and Optical Properties of Nanoporous Silicon at Terahertz Frequencies," Optical Materials Express, 4(2), 300-307 (2014).
- [33] L. V. Titova, T. L. Cocker, S. Xu *et al.*, "Ultrafast carrier dynamics and the role of grain boundaries in polycrystalline silicon thin films grown by molecular beam epitaxy," Semiconductor Science and Technology, 31(10), 105017 (2016).
- [34] C. Li, L. Huang, G. P. Snigdha *et al.*, "Role of Boundary Layer Diffusion in Vapor Deposition Growth of Chalcogenide Nanosheets: The Case of GeS," ACS Nano, 6(10), 8868-8877 (2012).
- [35] K. J. Koski, C. D. Wessells, B. W. Reed *et al.*, "Chemical Intercalation of Zerovalent Metals into 2D Layered Bi2Se3 Nanoribbons," Journal of the American Chemical Society, 134(33), 13773-13779 (2012).
- [36] K. P. Chen, F. R. Chung, M. Wang *et al.*, "Dual Element Intercalation into 2D Layered Bi2Se3 Nanoribbons," Journal of the American Chemical Society, 137(16), 5431-5437 (2015).
- [37] J. B. Baxter, and G. W. Guglietta, "Terahertz spectroscopy," Anal Chem, 83(12), 4342-68 (2011).
- [38] J. B. Baxter, and C. A. Schmuttenmaer, "Conductivity of ZnO nanowires, nanoparticles, and thin films using time-resolved terahertz spectroscopy," Journal of Physical Chemistry B, 110(50), 25229-25239 (2006).
- [39] N. Smith, "Classical generalization of the Drude formula for the optical conductivity," Physical Review B, 64(15), (2001).
- [40] T. L. Cocker, D. Baillie, M. Buruma *et al.*, "Microscopic origin of the Drude-Smith model," Physical Review B, 96(20), 205439 (2017).
- [41] P. Parkinson, J. Lloyd-Hughes, Q. Gao *et al.*, "Transient Terahertz Conductivity of GaAs Nanowires," Nano Letters, 7(7), 2162-2165 (2007).

- [42] D. G. Cooke, A. Meldrum, and P. Uhd Jepsen, "Ultrabroadband terahertz conductivity of Si nanocrystal films," Applied Physics Letters, 101(21), 211107 (2012).
- [43] Q.-l. Zhou, Y. Shi, B. Jin *et al.*, "Ultrafast Carrier Dynamics and Terahertz Conductivity of Photoexcited GaAs Under Electric Field," Applied Physics Letters, 93(10), 102103 (2008).
- [44] B. G. Alberding, P. A. DeSario, C. R. So *et al.*, "Static and Time-Resolved Terahertz Measurements of Photoconductivity in Solution-Deposited Ruthenium Dioxide Nanofilms," Journal of Physical Chemistry C, 121(7), 4037-4044 (2017).
- [45] C. E. P. Villegas, A. R. Rocha, and A. Marini, "Electron-phonon scattering effects on electronic and optical properties of orthorhombic GeS," Physical Review B, 94(13), 134306 (2016).
- [46] B. W. Reed, D. R. Williams, B. P. Moser *et al.*, "Chemically Tuning Quantized Acoustic Phonons in 2D Layered MoO3 Nanoribbons," Nano Letters, 19(7), 4406-4412 (2019).